Chinese Journal of Aeronautics, 2013,26(2): 470–480

Chinese Society of Aeronautics and Astronautics
& Beihang University

Chinese Journal of Aeronautics

cja@buaa.edu.cn
www.sciencedirect.com

Matching design of hydraulic load simulator with aerocraft actuator

Shang Yaoxing *, Yuan Hang, Jiao Zongxia, Yao Nan

Science and Technology on Aerocraft Control Laboratory, School of Automation Science and Electrical Engineering, Beihang University, Beijing 100191, China

Received 16 February 2012; revised 21 March 2012; accepted 25 April 2012
Available online 7 March 2013

KEYWORDS

Aerocraft actuator;
Design;
Flight simulation;
Hydraulic drive and control;
Hydraulic load simulator (HLS);
Matching;
Servo control;
Stiffness

Abstract This paper intends to provide theoretical basis for matching design of hydraulic load simulator (HLS) with aerocraft actuator in hardware-in-loop test, which is expected to help actuator designers overcome the obstacles in putting forward appropriate requirements of HLS. Traditional research overemphasizes the optimization of parameters and methods for HLS controllers. It lacks deliberation because experimental results and project experiences indicate different ultimate performance of a specific HLS. When the actuator paired with this HLS is replaced, the dynamic response and tracing precision of this HLS also change, and sometimes the whole system goes so far as to lose control. Based on the influence analysis of the preceding phenomena, a theory about matching design of aerocraft actuator with HLS is presented, together with two paired new concepts of "Standard Actuator" and "Standard HLS". Further research leads to seven important conclusions of matching design, which suggest that appropriate stiffness and output torque of HLS should be carefully designed and chosen for an actuator. Simulation results strongly support that the proposed principle of matching design can be anticipated to be one of the design criteria for HLS, and successfully used to explain experimental phenomena and project experiences.

1. Introduction

Hydraulic load simulators (HLS) have found wide applications in testing and hardware-in-loop simulation in the research of flap servo actuators of aerocraft flight control systems. As a typical torque servo system with strong motion disturbance, HLS is mainly used to load an aerodynamic torque on an aerocraft position servo actuator.[1,2]

Assembly of HLS unit is composed by torque sensor, hydraulic vane motor and its torque servo system. Structure of a typical hardware-in-loop load simulator for aerocraft test is shown in Fig. 1 with three parts: (1) hydraulic cylinder driving aerocraft angle control actuator, about which mounted stiffness factor of cylinder body is considered. (2) flap with inertia, elasticity and viscosity load. (3) HLS, which is stiffly connected with the actuator. The precise complex model of HLS is shown in Appendix A.

Traditional researchers in HLS domain always focus on the optimization of control parameters with an actuator[3–10] and

* Corresponding author. Tel.: +86 10 82338910.
E-mail address: syx@buaa.edu.cn (Y. Shang).

Peer review under responsibility of Editorial Committe of CJA.

ELSEVIER Production and hosting by Elsevier

1000-9361 © 2013 Production and hosting by Elsevier Ltd. on behalf of CSAA & BUAA. Open access under CC BY-NC-ND license.
http://dx.doi.org/10.1016/j.cja.2013.02.026

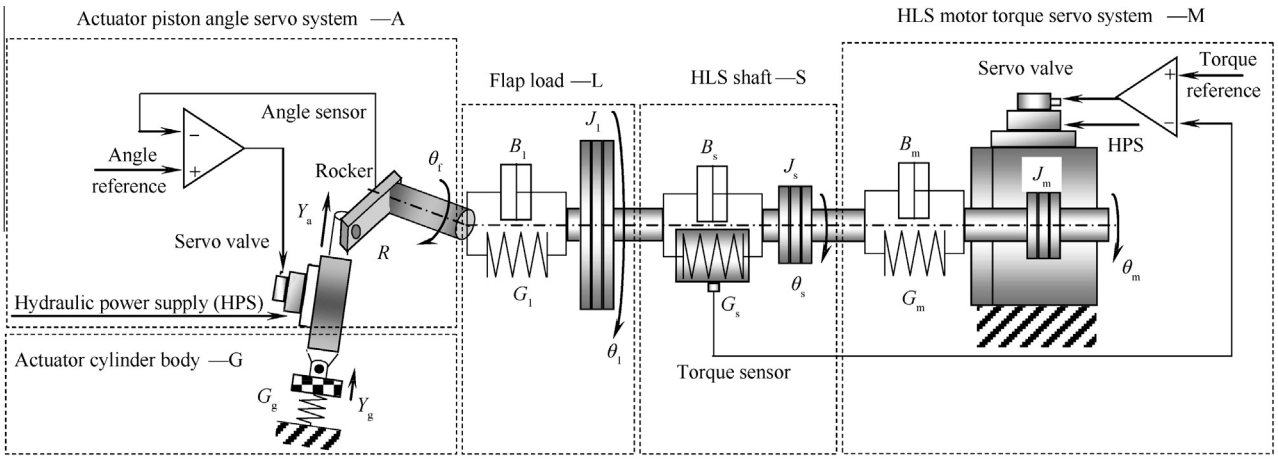

Fig. 1 Structure of a typical hardware-in-loop load simulator for aerocraft test.[1]

the improvement of nonlinear suppression.[11–13] Experimental results and project experiences indicate different ultimate performances of a HLS: performance of HLS does not remain the same with different actuators. When we replaced the actuator with another one, the dynamic response and tracing precision of HLS also changed. Sometimes the whole system goes so far as to lose control. We used a 600 N·m HLS to test the torque mode close loop frequency response (90° phase-lag) in three different states defined in Appendix D. The experimental result [1] of each state is excited by a 100 N·m swept sine reference of torque signal. In each state, the parameters of HLS controller have been optimized to obtain the best performance. In static locked-rotor state, the response data is no less than 80 Hz; in self-calibration state, it is 80 Hz; with a 300 N·m actuator, it decreases to 50 Hz.

This phenomenon indicates that different statuses and actuators bring non-identical effects to the HLS. Thus we focused on the influence of aerocraft actuator on HLS in Ref.,[1] in which some principles and conclusions of this influence were analyzed and presented in the form of mathematic transfer function, which related to the load stiffness of aerocraft actuator.

Based on the influence principle, this paper focuses on matching design of HLS with aerocraft actuator. We try to provide the basis and conclusions for matching design, which are expected to overcome the difficulties to put forward the appropriate performance requirements of HLS in hardware-in-loop test for actuator designers.

In Section 2, this paper begins to hit the high spots of principles and conclusions concerned with the influence of actuator on HLS presented in Ref.[1] In Section 3, a set of theoretical principles on the basis of further research in matching problems about HLS with actuator are proposed. In Section 4, the principles of matching design are examined and certified by the fact that simulation results are in concordance with experimental phenomena and experience. A series of important conclusions listed in Section 5 provides the foundation for matching design of HLS with actuator. The paper ends up with drawing some conclusions in Section 6.

2. Principle of influence of actuator on HLS[1]

Conventional HLS research[8,14] suggests that the angle output θ_f (All of the notations are explained in Appendix C) of actuator is an independent motion disturbance of HLS, and the superposition principle can be applied since θ_f is orthogonal with all the state variables of HLS. Traditional HLS model has two kinds of input of spool displacement servo valve x_{vm} and θ_f, and its torque mode could be considered as the static locked-rotor status while $\theta_f = 0$. But in fact, it is not the truth when the dynamic stiffness[15–17] of actuator position control is considered.

Actuator is a typical position control system with time-variant torque disturbance load.[18] The dynamic flexibility Φ_a and stiffness γ_a of actuator in close loop mode are defined in transfer function as

$$\Phi_a(S) = \frac{\theta_f}{M_l} = \frac{1}{\gamma_a(S)}. \tag{1}$$

Note that actuator with higher stiffness and lower flexibility can bear stronger load disturbance while Φ_a and stiffness γ_a are negative.

$G_a(S)$ is close loop transfer function of actuator and $M_l = G_l(\theta_f - \theta_l)$is the time-variant load disturbance of actuator. Then the model of actuator is

$$\theta_f = G_a(S)\theta_r + \frac{1}{\gamma_a(S)} M_l \tag{2}$$

It is indicated in Eq. (2) that θ_f is not orthogonal or independent but related to some state variables of HLS, so the influence of HLS on actuator is verified by $G_a(S)$ and $\gamma_a(S)$. Yet angle reference signal θ_r of actuator is the output of flight control computer, which is orthogonal with system state variables. And θ_r must be used as the independent motion disturbance of HLS according to the superposition principle in model research.

Deduced from Eq. (2) and Eqs. (A12) and (A13) in Appendix A, the new model of HLS-Actuator system is

$$M_m = \frac{\left\{\left[\frac{1}{G_l} - \frac{1}{\gamma_a(S)}\right] J_l S^2 + \left[\frac{1}{G_l} - \frac{1}{\gamma_a(S)}\right] B_l S + 1\right\} \frac{D_m K_{Qm}}{K_{tm}} \left(\frac{J_l}{G_l} S^2 + \frac{B_l}{G_l} S + 1\right) x_{vm} - \left(\frac{J_l}{G_l} S^2 + \frac{B_l}{G_l} S + 1\right) G_a(S) N_m(S) S \theta_r}{\left\{\left[\frac{1}{G_l} - \frac{1}{\gamma_a(S)}\right] J_l S^2 + \left[\frac{1}{G_l} - \frac{1}{\gamma_a(S)}\right] B_l S + 1\right\} D_f(S) - \frac{1}{\gamma_a(S)} N_m(S) S} \tag{3}$$

Given:

$$\frac{1}{G_l}-\frac{1}{\gamma_a(S)}=\frac{1}{\Omega(S)} \tag{4}$$

where $\Omega(S)$ is considered as a combined stiffness of G_l and γ_a. Then Eq. (3) is converted into

$$M_m=\frac{\left(\frac{J_l}{\Omega(S)}S^2+\frac{B_l}{\Omega(S)}S+1\right)\frac{D_m K_{Qm}}{K_{tm}}\left(\frac{J_l}{G_l}S^2+\frac{B_l}{G_l}S+1\right)x_{vm}-\left(\frac{J_l}{G_l}S^2+\frac{B_l}{G_l}S+1\right)G_a(S)N_m(S)S\theta_r}{\left(\frac{J_l}{\Omega(S)}S^2+\frac{B_l}{\Omega(S)}S+1\right)D_f(S)-\frac{1}{\gamma_a(S)}N_m(S)S} \tag{5}$$

Since θ_r is the independent motion disturbance of HLS, two open loop transfer functions can be separated from Eq. (5) by applying the superposition principle. First, the open loop transfer function of HLS from spool displacement x_{vm} of servo valve to output M_m of torque sensor can be obtained as

$$\frac{M_m}{x_{vm}}=\frac{\left(\frac{J_l}{\Omega(S)}S^2+\frac{B_l}{\Omega(S)}S+1\right)\frac{D_m K_{Qm}}{K_{tm}}\left(\frac{J_l}{G_l}S^2+\frac{B_l}{G_l}S+1\right)}{\left(\frac{J_l}{\Omega(S)}S^2+\frac{B_l}{\Omega(S)}S+1\right)D_f(S)-\frac{1}{\gamma_a(S)}N_m(S)S}. \tag{6}$$

Second, the open loop transfer function of HLS against stronger motion disturbance from the reference signal θ_r of actuator angle to output M_m of torque sensor can be obtained as

$$\frac{M_m}{\theta_r}=\frac{-\left(\frac{J_l}{G_l}S^2+\frac{B_l}{G_l}S+1\right)G_a(S)N_m(S)S}{\left(\frac{J_l}{\Omega(S)}S^2+\frac{B_l}{\Omega(S)}S+1\right)D_f(S)-\frac{1}{\gamma_a(S)}N_m(S)S}. \tag{7}$$

From the principle of this influence in the form of transfer function shown in Eqs. (6) and (7), we can reach two conclusions.

Conclusion 1[1] Influence of actuator on HLS torque dynamic response

It is indicated by Eq. (6) that the open loop transfer function of HLS is directly influenced by actuator dynamic stiffness γ_a through the combined stiffness $\Omega(S)$. The characteristic of actuator dynamic stiffness can be considered as a variable mechanical spring which can filter the dynamic response of HLS system. If the actuator dynamic stiffness is the lowest one of all the stiffness factors, then the ultimate performance of HLS is determined by actuator. The transfer function of HLS seems to establish no relation with close loop transfer function $G_a(S)$ of actuator; however the zeros of γ_a and the poles of $G_a(S)$ are the same, as the numerator of γ_a equals the denominator of $G_a(S)$. Thus the close loop poles of actuator will influence HLS together with other factors.

Conclusion 2[1] Influence of actuator on HLS torque tracing precision against motion disturbance

Both dynamic stiffness γ_a and close loop transfer function $G_a(S)$ of actuator can affect the open loop transfer function of HLS against stronger motion disturbance and decide the original surplus force. If γ_a and $G_a(S)$ of the actuator change, then the controller parameters against disturbance of HLS need to be adjusted.

3. Matching relationship and principles about HLS with actuator

In order to explain the matching principles about HLS with actuator better, mathematical description is given. Considering the complexity of Eq. (5), as well as its subsequent inconvenient derivation and analysis, conventional simple model of HLS shown in Appendix B is analyzed instead of the influence model built in Section 4.

To obtain $M_m = f_r(x_{vm},\theta_r)$, solve Eq. (B5), Eq. (A12), Eq. (2) and $M_l = G_l(\theta_f - \theta_l)$ simultaneously like the derivation of Eq. (3), meanwhile, by applying the special combined stiffness $\Omega(S)$ defined in Eq. (4), there is

$$\frac{1}{G_l}-\frac{1}{\gamma_a(S)}=\frac{1}{G_l}-\Phi_a(S)=\frac{1}{\Omega(S)}$$

Then,

$$M_m=\frac{\frac{D_m K_{Qm}}{K_{tm}}\left(\frac{J_l}{G_l}S^2+\frac{B_m}{G_l}S+1\right)\left(\frac{J_l}{\Omega(S)}S^2+\frac{B_m}{\Omega(S)}S+1\right)x_{vm}-\frac{D_m^2}{K_{tm}}S\left(\frac{J_l}{G_l}S^2+\frac{B_m}{G_l}S+1\right)G_a(S)\theta_r}{\left(\frac{J_l}{\Omega(S)}S^2+\frac{B_m}{\Omega(S)}S+1\right)\left[\left(\frac{V_m}{4E_y K_{tm}}S+1\right)\left(\frac{J_l}{G_l}S^2+\frac{B_m}{G_l}S+1\right)+\frac{D_m^2}{K_{tm}G_l}S\right]-\frac{D_m^2}{K_{tm}\gamma_a(S)}S} \tag{8}$$

The Eq. (8) can be transformed to

$$M_m=\frac{\frac{D_m K_{Qm}}{K_{tm}}\left(\frac{J_l}{G_l}S^2+\frac{B_m}{G_l}S+1\right)x_{vm}-\frac{D_m^2}{K_{tm}}S\frac{\left(\frac{J_l}{G_l}S^2+\frac{B_m}{G_l}S+1\right)}{\left(\frac{J_l}{\Omega(S)}S^2+\frac{B_m}{\Omega(S)}S+1\right)}G_a(S)\theta_r}{\left(\frac{V_m}{4E_y K_{tm}}S+1\right)\left(\frac{J_l}{G_l}S^2+\frac{B_m}{G_l}S+1\right)+\left(1-\frac{G_l/\gamma_a(S)}{\frac{J_l}{\Omega(S)}S^2+\frac{B_m}{\Omega(S)}S+1}\right)\frac{D_m^2}{K_{tm}G_l}S}. \tag{9}$$

Let

$$\varepsilon_N=\frac{\left(\frac{J_l}{G_l}S^2+\frac{B_m}{G_l}S+1\right)}{\left(\frac{J_l}{\Omega(S)}S^2+\frac{B_m}{\Omega(S)}S+1\right)}G_a(S) \tag{10}$$

and

$$\varepsilon_D=-\frac{G_l/\gamma_a(S)}{\frac{J_l}{\Omega(S)}S^2+\frac{B_m}{\Omega(S)}S+1}. \tag{11}$$

Then, Eq. (9) is converted into

$$M_m=\frac{\frac{D_m K_{Qm}}{K_{tm}}\left(\frac{J_l}{G_l}S^2+\frac{B_m}{G_l}S+1\right)x_{vm}-\varepsilon_N\frac{D_m^2}{K_{tm}}S\theta_r}{\left(\frac{V_m}{4E_y K_{tm}}S+1\right)\left(\frac{J_l}{G_l}S^2+\frac{B_m}{G_l}S+1\right)+(1+\varepsilon_D)\frac{D_m^2}{K_{tm}G_l}S} \tag{12}$$

According to the superposition principle, two open loop transfer functions can be separated from Eq. (12). First, the open loop transfer function of HLS from spool displacement servo valve x_{vm} to output of torque sensor M_m is

$$\frac{M_m}{x_{vm}}=\frac{\frac{D_m K_{Qm}}{K_{tm}}\left(\frac{J_l}{G_l}S^2+\frac{B_m}{G_l}S+1\right)}{\left[\left(\frac{V_m}{4E_y K_{tm}}S+1\right)\left(\frac{J_l}{G_l}S^2+\frac{B_m}{G_l}S+1\right)+\frac{D_m^2}{K_{tm}G_l}S\right]+(1+\varepsilon_D)\frac{D_m^2}{K_{tm}G_l}S} \tag{13}$$

Second, the open loop transfer function against stronger motion disturbance from the actuator angle reference signal θ_r to output of torque sensor M_m is

$$\frac{M_m}{\theta_r}=\frac{-\varepsilon_N\frac{D_m^2}{K_{tm}}S}{\left(\frac{V_m}{4E_yK_{tm}}S+1\right)\left(\frac{J_l}{G_l}S^2+\frac{B_m}{G_l}S+1\right)+(1+\varepsilon_D)\frac{D_m^2}{K_{tm}G_l}S} \tag{14}$$

Two conclusions can be reached by comparing Eq. (12) with non-actuator form Eq. (B5).

Conclusion 3 The influence of actuator on denominator polynomial of HLS transfer functions is indicated by an extra ε_D factor, which is only related to close loop stiffness of actuator. It can be determined from the definition of ε_D that $\varepsilon_D \to 0$ when running without actuator, because $|\gamma_a(S)|$ is infinite, and according to the definition of $\Omega(S)$, $\Omega(S) \to G_l$. Then HLS transfer function described by Eq. (13) is one without actuator. After all, to reduce the effect of actuator on frequency characteristics of HLS, it is required that

$$\varepsilon_D \ll 1 \tag{15}$$

Conclusion 4 The influence of actuator on the motion disturbance term of numerator polynomial of HLS transfer functions is indicated by an extra ε_D factor, which is related to both load close loop stiffness and frequency response of actuator. It can be determined from the definition of ε_N (Eq. (10)) that $\varepsilon_N \to 1$ when running without actuator, because $|\gamma_a(S)|$ is infinite, $\theta_f = \theta_r$, that is $G_a(S) = 1$, and likewise $\Omega(S) \to G_l$. Then HLS transfer function described by Eq. (14) is one without actuator.

Equations and derivations about the influence of actuator on HLS in Section 4 are confirmed by the last two conclusions.

As to the simple model for HLS applied in this section, load stiffness G_l is a generalized concept. To be more exact, it should be interpreted as comprehensive mechanical stiffness G_t of HLS, which is converted by the lumped-mass method. G_t includes connection stiffness of actuator and HLS as well as the stiffness of other mechanical elements of HLS, and it can also be reflected by the maximal output torque of HLS. With regard to the multiple stiffness model in Appendix A, G_t is the combination of G_l, G_s and G_m, that is

$$\frac{1}{G_t}=\frac{1}{G_l}+\frac{1}{G_s}+\frac{1}{G_m}. \tag{16}$$

Likewise, load inertia in the simple model is also a generalized lumped-inertia concept. It is actually the equivalent total mechanical inertia of HLS, that is

$$J_t = J_l + J_s + J_m. \tag{17}$$

Thus, these two concepts of HLS, comprehensive mechanical stiffness G_t and equivalent total mechanical inertia J_t, are applied to the discussion below.

Observation of the determined Eq. (11) of ε_D leads to the following important conclusions.

Conclusion 5 If the matching relationship between comprehensive mechanical stiffness G_t of a HLS and static load stiffness $|\gamma_{a0}|$ of an actuator is described as

$$G_t/|\gamma_{a0}| \leqslant 0.05 \tag{18}$$

then the influence of this actuator on the HLS is negligible and this set of actuator and HLS are individually matched to each other. In addition, if the maximal torque of actuator approximates to that of HLS, this actuator will be regarded as Standard Actuator of the HLS, and this HLS shall be regarded as Standard HLS of the actuator.

In this case, frequency response of HLS with actuator approximates to that in static locked-rotor status without actuator. It means the close loop frequency response of HLS in static locked-rotor status can represent the loading capability of Standard Actuator. This frequency response of HLS in static locked-rotor status can be compared with requirements to regulate the design.

Explanation for Conclusion 5 When G_t is much less than $|\gamma_a|$, namely $G_t/|\gamma_{a0}| \leqslant 0.05$, $\Omega(S) \to G_l$. The oscillation element of $(J_lS^2/G_l + B_lS/G_l + 1)$ must be designed to be higher than the required bandwidth ω_{sm} of HLS, so that $\varepsilon_D \approx G_l/|\gamma_a| \leqslant 0.05$, which satisfies $\varepsilon_D \ll 1$ as demanded in Conclusion 3. Therefore ε_D has little influence on the open loop transfer function of HLS, and the static locked-rotor status can approximately represent this state with actuator. Then the influence of this actuator on the HLS is negligible.

Actually because of the difficulty of dynamic stiffness measurement, stiffness of actuator measured by manufacturers is usually static load stiffness. Thus γ_a can be replaced by γ_{a0} when compared with G_l, which leads to Eq. (18).

4. Simulation of matching principles of HLS with actuator

In order to simulate the influence of actuator on HLS firstly, an HLS with its maximal torque 2300 N·m is considered to be the subject investigated, and all its parameters are shown in Table 2 of Ref.[1]

A 1600 N·m actuator with parameters in Table 3 of Ref.[1] and a 40 N·m actuator with parameters in Table 4 of Ref.[1] are compared when each of them is connected with the 2300 N·m HLS.

The 1600 N·m actuator bandwidth is 24.7 Hz. The 40 N·m actuator bandwidth is 79.2 Hz.[1]

The simulation results of absolute value of actuator's dynamic flexibility is shown in Fig. 2 as different actuators have

Table 1 Parameters of 60 N·m—600 (°)·s^{-1} HLS.

Notation	Unit	Value
$(M_m)_{max}$	N·m	60
$(Q_{fm})_{max}$	m^3·s^{-1}	1.667×10^{-4}
$(x_{vm})_{max}$	m	5×10^{-4}
$(i_m)_{max}$	A	0.04
B_l	N·m·s·rad^{-1}	0.04
B_m	N·m·s·rad^{-1}	0.04
B_s	N·m·s·rad^{-1}	0.04
D_m	m^3·rad^{-1}	5×10^{-6}
E_y	N·m^{-2}	1.372×10^{9}
G_l	N·m·rad^{-1}	8000
G_s	N·m·rad^{-1}	2000
G_m	N·m·rad^{-1}	4000
J_m	kg·m^2	5×10^{-5}
J_l	kg·m^2	5×10^{-4}
J_s	kg·m^2	5×10^{-5}
K_{fm}	V·N^{-1}·m^{-1}	0.1667
K_{Qm}	m^2·s^{-1}	0.5774
K_{sm}	m·A^{-1}	0.0125
K_{tm}	m^5·N^{-1}·s^{-1}	2.0373×10^{-12}
K_{vim}	A·V^{-1}	0.004
V_m	m^3	1.57×10^{-5}
ω_{sm}	rad·s^{-1}	1570.8

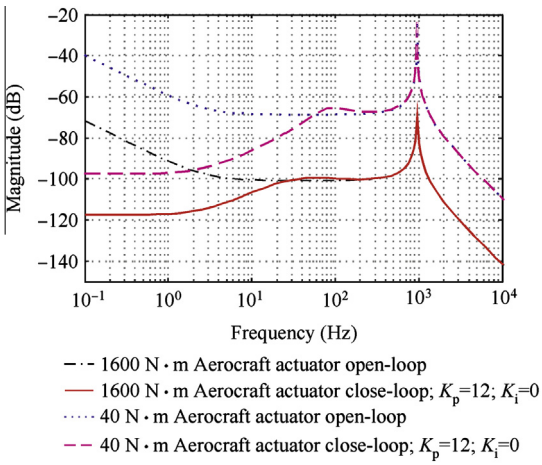

Fig. 2 Close loop and open loop magnitude frequency of actuator dynamic flexibility[1] (K_p and K_i are the parameters of close loop PI controller of actuator).

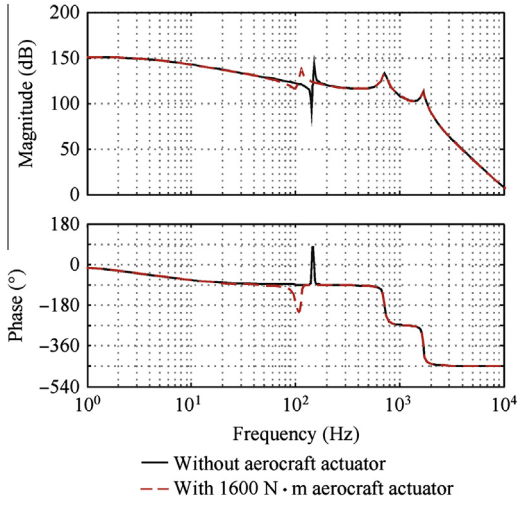

Fig. 3 Comparison of open loop frequency response of HLS with actuator and that without actuator.[1]

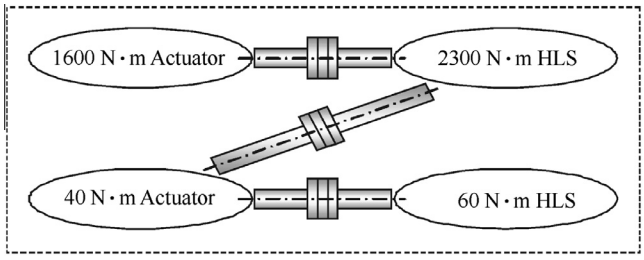

Fig. 4 Investigated subjects of matching relationship between actuator and HLS.

different close loop and open loop magnitude frequency characteristics of $|\gamma_a(S)|$. It is apparent that load stiffness of the 1600 N·m actuator is higher.[1]

The static load close loop stiffness of 1600 N·m actuator is calculated to be -3.3623×10^6 N·m·rad^{-1} and stiffness of 40 N·m actuator is -8.4057×10^4 N·m·rad^{-1}.[1]

Fig. 3 shows the open loop frequency response of HLS from spool displacement x_{vm} of HLS servo valve to output M_m of torque sensor. The solid line represents the HLS response in static locked-rotor mode when $\theta_f = 0$, while the broken line represents the HLS response with 1600 N·m actuator when $\theta_r = 0$.[1]

Fig. 3 indicates that the actuator can influence the resonance peak and reduce the speed of response due to the dynamic spring stiffness of actuator.[1]

Simulations in Ref.[1] also compared the open loop and close loop frequency response of HLS with different actuators to reproduce the experimental phenomenon.

To be convenient for research of matching design, another HLS under the maximal torque of 60 N·m and peak velocity of 600 (°)·s^{-1} is considered to be the subject investigated with parameters shown in Table 1.

The two different actuators mentioned above are simulated with these two types of HLS respectively, so that the matching relationship of these three different matched pairs of actuators and HLS shown in Fig. 4 can be investigated thoroughly: (1) 2300 N·m HLS—1600 N·m actuator; (2) 2300 N·m HLS—40 N·m actuator and (3) 60 N·m HLS—40 N·m actuator.

The investigation of matched pair 60 N·m HLS—1600 N·m actuator is meaningless so that it is abandoned.

Validation procedures of Conclusion 5 Comprehensive mechanical stiffness G_t of each HLS can be obtained from Eq. (16) as follows.

(1) For 2300 N·m HLS

$$G_t = 5.714\times10^4 \tag{19}$$

(2) For 60 N·m HLS

$$G_t = 1.143\times10^3 \tag{20}$$

The relationships between γ_{a0} and G_t of these matched pairs are concluded as follows based upon parameters of the two actuators and two types of HLS, together with the two above equations and the two above static load close loop stiffness of two actuators.

(1) 2300 N·m HLS—1600 N·m actuator:

$$G_t/|\gamma_{a0}| = 5.714\times10^4/3.3623\times10^6 = 0.01699$$

(2) 2300 N·m HLS—40 N·m actuator:

$$G_t/|\gamma_{a0}| = 5.714\times10^4/8.4057\times10^4 = 0.6798$$

(3) 2300 N·m HLS—40 N·m actuator:

$$G_t/|\gamma_{a0}| = 1.143\times10^3/8.4057\times10^4 = 0.01360$$

Apparently, Eq. (18) is satisfied with matched pairs 2300 N·m HLS—1600 N·m actuator and 60 N·m HLS—40 N·m actuator, that is $G_t/|\gamma_{a0}| \leqslant 0.05 \ll 1$, so that according to Conclusion 5, the stiffness of actuator does not influence frequency response of HLS seriously under both conditions.

But as to the matched pair 2300 N·m HLS—40 N·m actuator, $G_t/|\gamma_{a0}|$ reaches up to 0.6798, and ε_D approaches 1. In

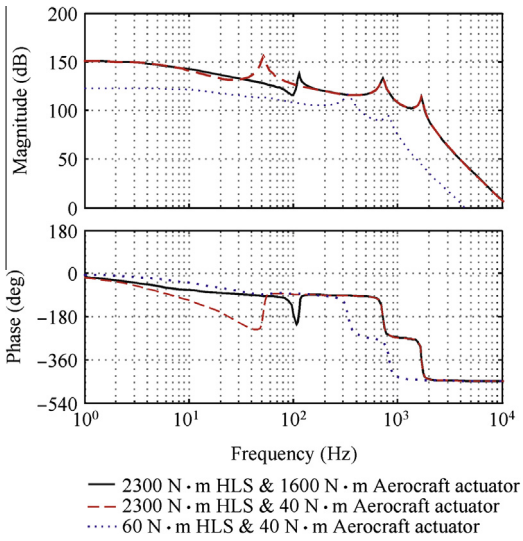

Fig. 5 Comparison of simulation results of three matched pairs of HLS and actuator.

other words, the actuator has a strong impact on HLS with great movement of its open loop poles affected by ε_D. The performance of 2300 N·m HLS, which has been well adjusted without actuator before, is not guaranteed any more.

To testify the analysis above, the open loop frequency response of HLS with actuator for each of these three matched pairs is simulated. The simulation curves are shown in Fig. 5.

Fig. 5 indicates that change of the actuator from 1600 N·m to 40 N·m with the HLS remaining 2300 N·m leads to a marked difference in open loop frequency response. The resonance peak reduces sharply to nearly 50 Hz, and stability phase margin drops badly.

After changing the HLS from 2300 N·m to 60 N·m with the actuator remaining 40Nm, in open loop magnitude-frequency curve, the resonant peak at 50 Hz disappears and gain is decreased in low-frequency range. The phase performance is also much better because the rapid lag in the low-frequency range below 40 Hz of phase frequency response also disappears and stability phase margin increases.

These simulation results have verified Conclusion 5. Both matching pairs 2300 N·m HLS—1600 N·m actuator and 60 N·m HLS—40 N·m actuator have desired performance; on the other hand, 2300 N·m HLS—40 N·m actuator can bring damage to the system.

5. Matching design of HLS with actuator

On the basis of the verified Conclusion 5, the following theoretical principles can be summarized to instruct the matching design of actuator and HLS.

Conclusion 6: When pair up an HLS with a variety of actuators, make sure that maximal output torque of these actuators approximates to but not much less than this HLS, and meets the requirements in Conclusion 5, or it must be replaced by another suitable HLS.

It is recommended that the torque redundancy of HLS should be appropriate, that is the torque of HLS should be either the same with actuator or slightly larger. It is not correct to cover a wide range of actuators in terms of the maximal loading torque for an oversize HLS does not complement a small actuator perfectly.

Explanation for Conclusion 6: Conclusion 5 helps to determine if an HLS matches an actuator. As a matter of fact, the static stiffness of actuator $|\gamma_{a0}|$ is already known, and the comprehensive mechanical stiffness G_t is adjustable in design. With a larger maximal output torque of HLS, the comprehensive mechanical stiffness G_t will also be larger, which implies a connection between the maximal output torque of HLS and Eq. (18) which proves Conclusion 6.

When we use an oversize HLS to a small torque actuator, the comprehensive mechanical stiffness G_t of HLS will decrease because of the thinner output shaft of actuator. The decrease of G_t compensates the stiffness degradation of actuator to a certain extent according to Eq. (18), but the decrease of the mechanical resonant frequency of HLS leads to a lower bandwidth of the whole system. Thus, it is not advisable to match a small torque actuator with an oversize HLS.

In traditional philosophy of HLS design, it is recommended to increase the mechanical resonant frequency $\Omega_{hl} = \sqrt{G_t/J_t}$ as much as possible, so that G_t is tried to increase as far as possible with the total inertia J_t fixed.[15] The mechanical resonant frequency should be larger than the required bandwidth of HLS with some relative margins. Based on lots of project experiences in HLS design, the margins is needed to be at least 20% to ensure the closed-loop system stability in expected bandwidth, so that is

$$\Omega_{hl} = \sqrt{G_t/J_t} > 1.2\Omega_{mr} \tag{21}$$

where, $\omega_{mr} = 2\pi f_{mr}$.

Solve the equation right above with Eq. (18) simultaneously, then there comes the result as

$$1.44\Omega_{mr}^2 J_t < G_t \leqslant 0.05|\gamma_{a0}|, \tag{22}$$

in another form, that is

$$5.76\pi^2 f_{mr}^2 J_t < G_t \leqslant 0.05|\gamma_{a0}|. \tag{23}$$

By analyzing Eqs. (22) and (23), the following conclusion can be reached.

Conclusion 7: As for a specific actuator with bandwidth f_a (Hz) and inertia J_t, static stiffness $|\gamma_{a0}|$ (Nm·rad^{-1}), the matched standard HLS must satisfy the following performance.

Firstly, close loop bandwidth f_{mr} of the HLS and f_a of the actuator must satisfy the following relationship:

$$f_{mr} \geqslant 2f_a. \tag{24}$$

Secondly, substitute Eq. (24) into Eq. (23), then the comprehensive mechanical stiffness G_t of this standard HLS ought to satisfy the equation as follows.

$$23.04\pi^2 f_a^2 J_t < G_t \leqslant 0.05|\gamma_{a0}|. \tag{25}$$

The HLS designed by the rule shown as Eq. (25) must match this actuator.

Thirdly, frequency response of the designed HLS in static locked-rotor status can represent its characteristics with a real actuator.

Explanation and verification for Conclusion 7 The purpose of loading test is to inspect capability of actuator controller against load torque fluctuation. The fluctuation of load torque can result in changes of acceleration control loop of actuator. For hydraulic

actuator, the load pressure of cylinder can rapidly respond to the load fluctuation. Thus, HLS is required to reappear with the influence to load pressure of actuator cylinder, so that the HLS should have the same rapid frequency response as the acceleration control loop of actuator at least. The bandwidth of internal acceleration control loop of a normal position control actuator must be larger than twice of the bandwidth of external position control loop, as confirmed in Eq. (24).

To testify Eq. (25), the following numerical operations with two kinds of actuator are performed.

(1) 1600 N·m actuator

The bandwidth of the 1600 N·m actuator is 24.7 Hz,[1] so according to its calculated stiffness $\gamma_{a0} = -3.3623 \times 10^6$ N·m·rad^{-1}, the bandwidth of Standard HLS of this actuator from Eq. (24) is

$$f_{mr} \geqslant 2 \times 24.7 = 49.4 \text{ Hz}$$

From Eq. (25), there is

$$7.145 \times 10^4 < G_t \leqslant 1.6815 \times 10^5.$$

The value of G_t of the 2300 N·m HLS calculated in Eq. (19) is 5.714×10^4 N·m·rad^{-1}, which falls outside the range of inequation above. The 1600 N·m actuator will affect this HLS a little bit, which dovetails with the simulation results in Fig. 3. An adequate Standard HLS for 1600 N·m actuator should have a bandwidth larger than 49.4 Hz and meet the stiffness condition above, so that comprehensive shaft stiffness G_t of the 2300 N·m HLS need to be enhanced.

(2) 40 N·m actuator

The bandwidth of the 40 Nm actuator is 79.2 Hz,[1] so according to its calculated stiffness $\gamma_{a0} = -8.4057 \times 10^4$ N·m·rad^{-1}, the bandwidth of Standard HLS of this actuator from Eq. (24) is

$$f_{mr} \geqslant 2 \times 79.2 = 158.4 \text{ Hz}$$

From Eq. (25), there is

$$0.8558 \times 10^3 < G_t \leqslant 4.203 \times 10^3$$

The value of G_t of the 60 N·m HLS calculated in Eq. (20) is 1.143×10^4 N·m·rad^{-1}, which falls within the range of inequation above. So the 60 N·m HLS with parameters shown in Table 1 is the Standard HLS for 40 N·m actuator.

Supplement for Conclusion 7 Theoretically, comprehensive mechanical stiffness G_t of HLS could be infinitely great by designer, not to mention breaking the limit of $0.05|\gamma_{a0}|$, and the stiffness of this HLS can be ultrahigh. This theory is not in contradiction with the theories in this paper, since it only indicates that the actuator with stiffness $|\gamma_{a0}|$ is not the Standard Actuator for this HLS with ultrahigh stiffness. Moreover, bandwidth of the HLS with this actuator will plummet even if bandwidth of the HLS is larger than 300 Hz in static locked-rotor status.

In other words, frequency response of HLS is limited by the performance of actuator. It is inadvisable to increase G_t blindly when the inertia is required to be fixed, because this will not only lead to cost increase, but also break up the matching relationship between HLS and actuator. Actuator becomes the major factor that influences system performance, so frequency response of the actuator-HLS system can never reach the level of that in static locked-rotor status.

6. Conclusions

Based on the phenomena which reveal the influence of actuator on HLS, this paper intends to probe into the nature of the influence. After analyzing and illustrating the influence principles of actuator on HLS by stiffness, systematic investigations into the matching problems about HLS with actuator propose a set of principles which will contribute to the matching design process. Several research conclusions are reached as follows.

(1) Open loop frequency response of HLS is seriously influenced by dynamic stiffness of actuator, so is the stability of HLS. Dynamic stiffness is one of the major factors that have effects on the ultimate performance of the whole system, for the resonant frequency formed by actuator stiffness is the lowest one of the whole system.
(2) The open loop transfer function of HLS against stronger motion disturbance is influenced by both dynamic stiffness and frequency response of actuator. To put it another way, the original surplus-force is decided by the same two factors. The controller with surplus-force eliminated must be adjusted after changing actuator.
(3) If the comprehensive mechanical stiffness of HLS is less than 5% of the static stiffness of actuator, then the influence of actuator on HLS is negligible and they are individually matched to each other. In addition, if the maximal torque of actuator approximates to that of HLS, this actuator will be regarded as Standard Actuator of HLS, and this HLS shall be regarded as Standard HLS of the actuator. Frequency response of HLS in static locked-rotor status can be used to compare with the requirement to regulate the design.
(4) When pair up a HLS with a variety of actuators, make sure that the maximal output torque of these actuators approximates to but not much less than this HLS, or it must be replaced by another suitable HLS. It is recommended that the torque redundancy of HLS should be appropriate. It is not correct to cover a wide range of actuators in terms of maximal loading torque for an oversize HLS does not complement a small actuator perfectly.
(5) As for a specific actuator, a matched HLS can be designed based on the conclusions given by this paper. Frequency response of the well-designed HLS in static locked-rotor status can represent its characteristics with a real actuator because it is easy to be measured.

Acknowledgements

The authors would like to express their gratitude to the Aviation Science Foundation (No. 20110951009) of China and National Nature Science Foundation for Distinguished Young Scholars (No. 50825502) of China for the financial support.

Appendix A. The precise multiple stiffness complex model of HLS

Suppositions are made as Ref.[19] based on the structure of HLS shown in Fig. 1. The precise multiple stiffness complex model of HLS is as follows:[20]

The model of flap load—L is

$$G_l(\theta_f-\theta_l)=J_lS^2\theta_l+B_lS\theta_l+G_s(\theta_l-\theta_s) \tag{A1}$$

The model of HLS shaft—S is

$$G_s(\theta_l-\theta_s)=J_sS^2\theta_s+B_sS\theta_s+G_m(\theta_s-\theta_m) \tag{A2}$$

The model of hydraulic motor rotor—M of HLS is

$$D_mP_{fm}=J_mS^2\theta_m+B_mS\theta_m-G_m(\theta_s-\theta_m). \tag{A3}$$

The output of torque sensor can be used as the output of the whole HLS system, because the position of torque sensor is the point of aerodynamic torque loaded to the flap. In order to ensure that the gain of HLS torque tracing channel is positive, the torque output of motor is chosen to be

$$M_m=G_s(\theta_s-\theta_l). \tag{A4}$$

The load flow of HLS can be calculated by

$$Q_{fm}=D_mS\theta_m+\frac{V_m}{4E_y}Sp_{fm}+C_{slm}p_{fm}. \tag{A5}$$

The linearized flow equation of HLS servo valve is

$$Q_{fm}=K_{Qm}x_{vm}-K_{cm}p_{fm}. \tag{A6}$$

Let $K_{tm}=K_{cm}+C_{slm}$, from Eqs. (A1), (A2), (A3), (A4), (A5), (A6), the model of HLS in the form of $M_m=f_m(x_{vm},\theta_m)$ is described as

$$M_m=\frac{\frac{D_mK_{Qm}}{K_{tm}}\left(\frac{J_s}{G_m}S^2+\frac{B_s}{G_m}S+1\right)x_{vm}-N_m(S)S\theta_m}{\frac{V_m}{4E_yK_{tm}}S+1} \tag{A7}$$

where

$$\begin{aligned}N_m(S)=&\frac{J_sJ_mV_m}{4E_yK_{tm}G_m}S^4+\left[\frac{J_sJ_m}{G_m}+\frac{(J_sB_m+J_mB_s)V_m}{4E_yK_{tm}G_m}\right]S^3\\&+\left[\frac{(J_sB_m+J_mB_s)}{G_m}+\frac{D_m^2J_s}{K_{tm}G_m}+\frac{(J_sG_m+J_mG_m+B_mB_s)V_m}{4E_yK_{tm}G_m}\right]S^2\\&+\left[\frac{B_sB_m}{G_m}+\frac{D_m^2B_s}{K_{tm}G_m}+\frac{(B_m+B_s)V_m}{4E_yK_{tm}}+(J_s+J_m)\right]S\\&+\left(B_m+B_s+\frac{D_m^2}{K_{tm}}\right).\end{aligned}$$

With Eq. (A4), Eq. (A2) is converted into

$$\theta_m=g_m(\theta_s,M_m)=\left(\frac{J_s}{G_m}S^2+\frac{B_s}{G_m}S+1\right)\theta_s+\frac{1}{G_m}M_m \tag{A8}$$

The model of HLS in the form of $M_m=f_z(x_{vm},\theta_s)$ can be calculated as follows from Eq. (A7) and Eq. (A8),

$$M_m=\frac{\frac{D_mK_{Qm}}{K_{tm}}x_{vm}-N_m(S)\cdot S\theta_s}{D_s(S)} \tag{A9}$$

where

$$\begin{aligned}D_s(S)=&\frac{J_mV_m}{4E_yK_{tm}G_m}S^3+\left(\frac{J_m}{G_m}+\frac{B_mV_m}{4E_yK_{tm}G_m}\right)S^2\\&+\left(\frac{B_m}{G_m}+\frac{D_m^2}{G_mK_{tm}}+\frac{V_m}{4E_yK_{tm}}\right)S+1\end{aligned}$$

Eq. (A4) is converted into

$$\theta_s=g_s(\theta_l,M_m)=\theta_l+\frac{M_m}{G_s}. \tag{A10}$$

The model of HLS in the form of $M_m=f_l(x_{vm},\theta_l)$ can be described as follows from Eq. (A9) and Eq. (A10).

$$M_m=\frac{\frac{D_mK_{Qm}}{K_{tm}}x_{vm}-N_m(S)S\theta_l}{D_l(S)} \tag{A11}$$

where

$$D_l(s)=D_s(s)+\frac{N_m(S)\cdot S}{G_s}$$

With Eq. (A4), Eq. (A1) is converted into

$$\theta_l=g_l(\theta_f,M_m)=\frac{\theta_f+\frac{1}{G_l}M_m}{\frac{J_l}{G_l}S^2+\frac{B_l}{G_l}S+1} \tag{A12}$$

The model of HLS in the form of $M_m=f_f(x_{vm},\theta_f)$ can be described as follows from (A11)(A12).

$$M_m=\frac{\frac{D_mK_{Qm}}{K_{tm}}\left(\frac{J_l}{G_l}S^2+\frac{B_l}{G_l}S+1\right)x_{vm}-N_m(S)S\theta_f}{D_f(S)} \tag{A13}$$

where $D_f(S)=\left(\frac{J_l}{G_l}S^2+\frac{B_l}{G_l}S+1\right)D_l(S)+\frac{N_m(S)\cdot S}{G_l}$

Appendix B. The simple model of HLS

Based on the physical structure shown in Fig. B1, for the purpose of simplifying the model of HLS, suppositions are made as follows.[18]

The torsional stiffness of torque sensor is infinite; the angle of hydraulic motor equals that of the load and the torque output of motor equals the product of load pressure and radian displacement.[8]

For the above-cited typical actuating system with huge friction load, its torsional stiffness of load is far less than that of torque sensor, so the simplified model is precise enough to reflect the basic characteristics of HLS as follows:

The flow equation of servo valve is linearized into

$$Q_{fm}=K_{Qm}x_{vm}-K_{cm}p_{fm} \tag{B1}$$

The load flow continuity equation is described by

$$Q_{fm}=D_mS\theta_m+\frac{V_m}{4E_y}Sp_{fm}+C_{slm}p_{fm} \tag{B2}$$

The dynamic equation of hydraulic motor is described by

$$D_mp_{fm}=J_lS^2\theta_m+B_mS\theta_m+G_l(\theta_m-\theta_f) \tag{B3}$$

In order to ensure that the gain of loading system is positive, the torque output of motor is chosen to be

$$M_m=D_mp_{fm} \tag{B4}$$

Derived from Eqs. (B1), (B2), (B3), and (B4), the simple model of HLS is

$$M_m=\frac{\frac{D_mK_{Qm}}{K_{tm}}\left(\frac{J_l}{G_l}S^2+\frac{B_m}{G_l}S+1\right)x_{vm}-\frac{D_m^2}{K_{tm}}S\theta_f}{\left(\frac{V_m}{4E_yK_{tm}}S+1\right)\left(\frac{J_l}{G_l}S^2+\frac{B_m}{G_l}S+1\right)+\frac{D_m^2}{K_{tm}G_l}S} \tag{B5}$$

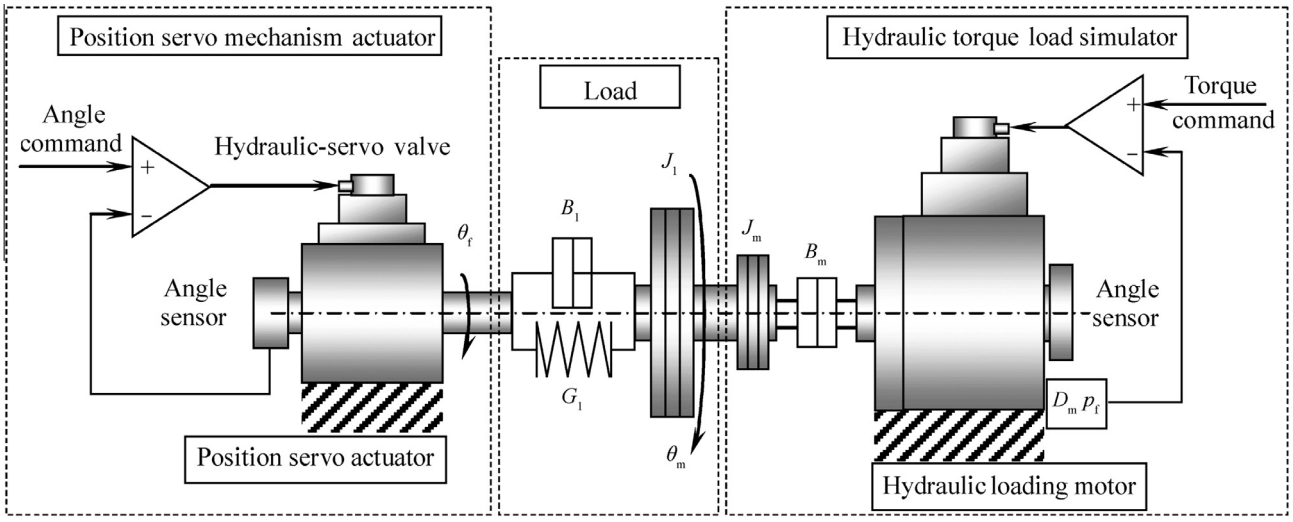

Fig. B1 Structure of HLS for simple model.[21]

in another form,

$$M_{\mathrm{m}}=\frac{\frac{D_{\mathrm{m}}K_{\mathrm{Qm}}}{K_{\mathrm{tm}}}\left(\frac{J_{\mathrm{l}}}{G_{\mathrm{l}}}S^2+\frac{B_{\mathrm{m}}}{G_{\mathrm{l}}}S+1\right)x_{\mathrm{vm}}-\frac{D_{\mathrm{m}}^2}{K_{\mathrm{tm}}}S\theta_{\mathrm{f}}}{\frac{J_{\mathrm{l}}V_{\mathrm{m}}}{4E_{\mathrm{y}}K_{\mathrm{tm}}G_{\mathrm{l}}}S^3+\left(\frac{B_{\mathrm{m}}V_{\mathrm{m}}}{4E_{\mathrm{y}}K_{\mathrm{tm}}G_{\mathrm{l}}}+\frac{J_{\mathrm{l}}}{G_{\mathrm{l}}}\right)S^2+\left(\frac{B_{\mathrm{m}}}{G_{\mathrm{l}}}+\frac{V_{\mathrm{m}}}{4E_{\mathrm{y}}K_{\mathrm{tm}}}+\frac{D_{\mathrm{m}}^2}{G_{\mathrm{l}}K_{\mathrm{tm}}}\right)S+1}. \tag{B6}$$

Appendix C. Notation

The parameters, variables and conditions this article involves are defined as follows: (see Table C1)

Table C1 Definition of notation.

	Definition	Unit
A_{t}	Piston area of actuator cylinder	m^2
B_{a}	Viscous damping of actuator cylinder piston	$\mathrm{N{\cdot}s{\cdot}m^{-1}}$
B_{l}	Effective viscous damping of flap load	$\mathrm{N{\cdot}m{\cdot}s{\cdot}rad^{-1}}$
B_{m}	Viscous damping of HLS motor rotor	$\mathrm{N{\cdot}m{\cdot}s{\cdot}rad^{-1}}$
B_{s}	Viscous damping of HLS shaft	$\mathrm{N{\cdot}m{\cdot}s{\cdot}rad^{-1}}$
C_{sla}	Leakage coefficient of actuator cylinder	$\mathrm{m^5{\cdot}N^{-1}{\cdot}s^{-1}}$
C_{slm}	Leakage coefficient of HLS hydraulic motor	$\mathrm{m^5{\cdot}N^{-1}{\cdot}s^{-1}}$
D_{m}	Radian displacement of HLS motor	$\mathrm{m^3{\cdot}rad^{-1}}$
E_{y}	Effective bulk modulus of hydraulic oil	Pa
f_{a}	Bandwidth of actuator	Hz
f_{mr}	Bandwidth of HLS	Hz
G_{g}	fixing stiffness of actuator cylinder block	$\mathrm{N{\cdot}m^{-1}}$
G_{l}	Effective torsion stiffness of the flap load	$\mathrm{N{\cdot}m{\cdot}rad^{-1}}$
G_{m}	Connection torsion stiffness between HLS shaft and hydraulic motor	$\mathrm{N{\cdot}m{\cdot}rad^{-1}}$
G_{s}	Torsion stiffness of torque sensor	$\mathrm{N{\cdot}m{\cdot}rad^{-1}}$
G_{t}	Comprehensive mechanical stiffness of HLS	$\mathrm{N{\cdot}m{\cdot}rad^{-1}}$
i_{a}	Driving current of actuator servo valve	A
i_{m}	Driving current of HLS servo valve	A
J_{l}	Effective inertia of flap load	$\mathrm{kg{\cdot}m^2}$
J_{m}	Rotor inertia of HLS hydraulic motor	$\mathrm{kg{\cdot}m^2}$
J_{s}	Inertia of HLS Shaft	$\mathrm{kg{\cdot}m^2}$
J_{t}	Equivalent total mechanical inertia of HLS	$\mathrm{kg{\cdot}m^2}$
K_{ca}	Whole factor of actuator servo valve of flow rate to pressure	$\mathrm{m^5{\cdot}N^{-1}{\cdot}s^{-1}}$
K_{cm}	Whole factor of HLS servo valve of flow rate to pressure	$\mathrm{m^5{\cdot}N^{-1}{\cdot}s^{-1}}$
K_{fa}	Feedback coefficient of angle	$\mathrm{V{\cdot}rad^{-1}}$
K_{fm}	Feedback coefficient of torque	$\mathrm{V{\cdot}N^{-1}{\cdot}m^{-1}}$
K_{Qa}	Flow rate gain of actuator servo valve	$\mathrm{m^2{\cdot}s^{-1}}$
K_{Qm}	Flow rate gain of HLS servo valve	$\mathrm{m^2{\cdot}s^{-1}}$
K_{sa}	Spool position gain of actuator servo valve	$\mathrm{m{\cdot}A^{-1}}$
K_{sm}	Spool position gain of HLS servo valve	$\mathrm{m{\cdot}A^{-1}}$
K_{via}	Gain of actuator servo valve current amplifier	$\mathrm{A{\cdot}V^{-1}}$

(*contined on next page*)

Table C1 (continued)

	Definition	Unit
K_{vim}	Gain of HLS servo valve current amplifier	$A \cdot V^{-1}$
M_m	Output of torque sensor	N·m
M_l	Variable disturbance load of actuator	N·m
M_r	Torque reference signal of HLS	N·m
m_a	Moving element mass of actuator cylinder piston	kg
m_g	Mass of actuator cylinder block	kg
p_{fm}	Load pressure of HLS	$N \cdot m^{-2}$
Q_{fa}	Load flow rate of actuator	$m^3 \cdot s^{-1}$
Q_{fm}	Load flow rate of HLS	$m^3 \cdot s^{-1}$
R	Length of actuator rocker	m
V_a	Total oil volume of actuator cylinder, servo valve and pipes	m^3
V_m	Total oil volume of HLS motor, servo valve and pipes	m^3
x_{va}	Spool displacement of actuator servo valve	m
x_{vm}	Spool displacement of HLS servo valve	m
Y_a	Displacement of actuator cylinder piston	m
Y_g	Displacement of actuator cylinder block	m
θ_f	Angle output of actuator	rad
θ_l	Angle of flap load	rad
θ_m	Angle of HLS hydraulic motor	rad
θ_r	Angle reference of actuator	rad
θ_s	Angle of torque sensor input shaft	rad
ω_{sa}	First order natural frequency of actuator servo valve	$rad \cdot s^{-1}$
ω_{sm}	First order natural frequency of HLS servo valve	$rad \cdot s^{-1}$
Φ_a	Close loop dynamic flexibility of actuator angle control	$rad \cdot N^{-1} \cdot m^{-1}$
γ_a	Close loop dynamic stiffness of actuator angle control	$rad \cdot N^{-1} \cdot m^{-1}$

Appendix D. Definition

(1) The torque direction is defined as follows: When the system moves forwards with a positive angle and at the same time if the load torque is of a resistance, the torque and the loading gradient are regarded to be positive.
(2) ''Static locked-rotor status'' means that the motion of HLS shaft is restricted to make $\theta_f = 0$.
(3) In ''self-calibration status'', another ectype of that HLS is running in angle control mode to simulate the real aerocraft actuator, while the HLS is stiffly connected to this dummy actuator. In other words, this status corresponds to test an actuator with the same maximal torque.
(4) In ''with real actuator'' status, HLS is stiffly connected with the actuator.

References

1. Shang YX, Jiao ZX, Yao N. Influence of aerocraft actuator on ultimate performance of Hydraulic Load Simulator. *Proceeding of 2011 international conference on fluid power and, mechatronics*; 2011. p. 850–6.
2. Jiao ZX. Review of the electro-hydraulic load simulator. *Proceeding of 8th Scandinavian international conference on fluid power*; 2003. p. 1–12.
3. Nam Y, Hong SK. Force control system design for aerodynamic load simulator. *Control Eng Pract* 2002;**10**(5):549–58.
4. Nam Y. QFT force loop design for the aerodynamic load simulator. *IEEE Trans Aerosp Electron Syst* 2001;**37**(4):1384–92.
5. AhnK YK, Truong DQ, Soo YH. Self tuning fuzzy PID control for hydraulic load simulator. *Proceeding of International conference on control, automation and systems*; 2007. p. 345–9.
6. Truong DQ, Kwan AK, Yoon JI. A Study on force control of electric-hydraulic load simulator using an online tuning quantitative feedback theory. *Proceeding of 2008 International conference on control, automation and systems*; 2008. p. 2622–7.
7. Truong DQ, Ahn KK. Force control for hydraulic load simulator using self-tuning grey predictor-fuzzy PID. *Mechatronics* 2009;**19**(2):233–46.
8. Hua Q. Studies on the key technology of electro-hydraulic load simulator [dissertation]. Beijing: Beijing University of Aeronautics and Astronautics; 2001 [Chinese].
9. Jiao ZX, Hua Q, Wang XD, Wang SP. Hybrid control on the electro-hydraulic load simulator. *Chin J Mech Eng* 2002;**38**(12):34–8 [Chinese].
10. Jiao ZX, Gao JX, Hua Q, Wang SP. The velocity synchronizing control on the electro-hydraulic load simulator. *Chin J Aeronaut* 2004;**17**(1):39–46.
11. Li GQ, Cao J, Zhang B, Zhao KD. Design of robust controller in electrohydraulic load simulator. *Proceedings of the 2006 international conference on machine learning and cybernetics*; 2006. p. 779–84.
12. Wang XD, Kang RJ. Analysis and compensation of the friction in force loading system based on electric cylinder. *Proceeding of 2nd inernational forum on system and mechatronics*; 2007. p. 229–34.
13. Shang YX, Jiao ZX, Wang SP, Wang XD. Dynamic robust compensation control to inherent high-frequency motion disturbance on the electro-hydraulic load simulator. *Int J Comput Appl Technol* 2009;**36**(2):117–24.
14. Wang ZL. *Hydraulic servo control*. Beijing: Beihang University Press; 1989 [Chinese].
15. Wu J, Zhang JS, Kang GH. Analysis and research of the impedance of hydraulic booster location system. *Sci Technol Eng* 2008;**8**(4):1124–8 [Chinese].
16. Wang HH, Wu J, Yuan CH. Analysis and research of the tester applied to test the impedance of hydraulic booster location system. *Hydraulics Pneumatics* 2004;**11**:1–3 [Chinese].

17. Wu J, Zhang JS, Kang GH. Simulation and modeling of the tester applied to test the impedance of hydraulic booster location system. *Mach Tool Hydraulics* 2008;**36**(7):134–6 [Chinese].
18. Liu CN. *The optimized design theory of hydraulic servo system*. Beijing: Metallurgical Industry Press; 1989 [Chinese].
19. Hua Q, Jiao ZX, Wang XD, Wang SP. Complex mathematical model of electro-hudraulic torque load simulator. *Chin J Mech Eng* 2002;**38**(11):31–5 [Chinese].
20. Shang YX, Wu S, Jiao ZX, Wang XD. Complex mathematical model of electro-hydraulic load simulator including multi-tiffness and nonlinear factors in ultimate performance research. *Acta Aeronaut Astronaut Sin* 2009;**30**(7):1331–40 [Chinese].
21. Shang YX, Jiao ZX, Wang XD, Zhao SJ. Study on friction torque loading with an electro-hydraulic load simulator. *Chin J Aeronaut* 2009;**22**(6):691–9.

Shang Yaoxing received the Ph.D. degree from Beihang University in 2009, and then became a lecturer there. His main research interests lie in mechatronics, aircraft hydraulic system and actuation system, as well as hydraulic load simulator.

Yuan Hang is a graduate student at School of Automation Science and Electrical Engineering, Beihang University, Beijing, China. She received her B.S. degree from Dalian Maritime University in 2012. Her area of research includes hydraulic servo control and multi-channel load simulation.

Jiao Zongxia is a professor, Ph.D. supervisor and dean at School of Automation Science and Electrical Engineering, Beihang University, Beijing, China. He received the Ph.D. degree from Zhejiang University in 1991. His current research interests are aircraft hydraulic system and actuation system, hydraulic servo control, and hydraulic servo components.

Yao Nan received the M.S. degrees from Beihang University in 2006, and then became a lecturer and Ph.D student there. Her main research interests lie in mechatronics and mathematical simulation.